Crystal Structures of the Recombinant Kringle 1 Domain of Human Plasminogen in Complexes with the Ligands ϵ-Aminocaproic Acid and *trans*-4-(Aminomethyl)cyclohexane-1-carboxylic Acid†

Irimpan I. Mathews,‡ Peggy Vanderhoff-Hanaver,‡ Francis J. Castellino,§ and Alexander Tulinsky*,‡

Department of Chemistry, Michigan State University, East Lansing, Michigan 48824, and Department of Chemistry and Biochemistry, University of Notre Dame, Notre Dame, Indiana 46556

Received September 7, 1995; Revised Manuscript Received December 18, 1995⊗

ABSTRACT: The X-ray crystal structures of the complexes of the recombinant kringle 1 domain of human plasminogen ($K1_{Pg}$) with the ligands ϵ-aminocaproic acid (EACA) and *trans*-4-(aminomethyl)cyclohexane-1-carboxylic acid (AMCHA), which are representative of a class of *in vivo* antifibrinolytic agents, have been determined at 2.1 Å resolution. Each $K1_{Pg}$/ligand unit cell contained a dimer of the complexes, and some small differences were noted in the kringle/ligand interatomic distances within the monomeric components of the dimers. The structures obtained allowed predictions to be made of the amino acid residues of $K1_{Pg}$ that are likely important to ligand binding. In the crystal structure, the anionic center of $K1_{Pg}$ responsible for coordinating the amino group of the ligands is composed of both Asp54 and Asp56, and the cationic center that stabilizes binding of the carboxylate moiety of the ligands is Arg70, with a possible contribution from Arg34. A hydrogen bond between the carboxylate of the ligand to the hydroxyl group of Tyr63 also appears to contribute to the kringle/ligand binding energies. The methylene groups of the ligand are stabilized in the binding pocket by van der Waals contacts with side-chain atoms of Trp61 and Tyr71. These conclusions are in general agreement with site-directed mutagenesis results that implicate many of the same amino acid residues in this binding process, thus showing that the crystal and solution structures are in basic accord with each other. Further comparisons of the X-ray crystal structures of the $K1_{Pg}$/ligand complexes with each other and with apo-$K1_{Pg}$ show that while small differences in $K1_{Pg}$ side-chain geometries may exist in the three structures, the binding pocket can be considered to be preformed in the apokringle and not substantially altered by the nature of the ω-amino acid ligand that is inserted into the site. From the similar geometries of the binding of EACA and AMCHA, it appears that the k_{on} is an important component to the tighter binding of AMCHA to $K1_{Pg}$, as compared to EACA. Ordered solvation effects of the bound AMCHA may contribute to its longer lifetime on $K1_{Pg}$, thereby retarding k_{off}, both effects thus accounting for the higher binding energy of AMCHA as compared to EACA.

Pg[1] is the plasma-derived zymogen of the serine protease Pm. This latter enzyme, which functions in dissolution of the blood clot, as well as in other cellular, epicellular, and pericellular events [for a review, see Castellino (1995)], consists of two polypeptide chains that are covalently linked by a pair of disulfide bonds. The heavy chain of Pm (561 amino acid residues) consists of five repeating homologous triple-disulfide-linked peptide regions, approximately 80 amino acid residues in length, termed "kringles" (Sottrup-Jensen et al., 1978). Similar structures are present in several other blood clotting and clot dissolving proteins, such as factor XII (McMullen & Fujikawa, 1985), prothrombin (Magnusson et al., 1975), tPA (Pennica et al., 1983), and UK (Steffens et al., 1982).

The kringle domains within these proteins are responsible for interactions of the intact proteins with regulators of their functional properties. In Pg and Pm, kringles that are currently known to display interactions with effector molecules include $K1_{Pg}$, $K2_{Pg}$, $K4_{Pg}$, and $K5_{Pg}$. The most widely investigated of these binding interactions is that of Pg with antifibrinolytic ω-amino acids, typified by L-lysine, EACA, and AMCHA. These effectors have relevance in protein−protein interactions. Specifically, the increasing ability of Pg to interact with Pm-digested fibrin, as compared to native fibrin, most likely occurs through kringle domain interactions with the carboxy-terminal lysine residues that are liberated consequent to Pm catalysis (Bok & Mangel, 1985). The ability of agents, such as EACA, to compete with Pg for its fibrin binding site(s), and thus displace Pg and Pm from the clot, is the mechanism that is most likely responsible for their *in vivo* antifibrinolytic effects. Additionally, Pg binding, mediated through the kringle domains, occurs with other plasma proteins, such as fibrinogen (Wiman & Wallen, 1977), histidine-rich glycoprotein (Lijnen et al., 1980), and α_2-antiplasmin (Moroi & Aoki, 1976). The latter interaction, as well as the strong binding of Pg to fibrin fragment E, is

† Supported by Grants HL-25942 (to A.T.) and HL-13423 (to F.J.C.) from the National Institutes of Health and by the Kleiderer/Pezold Family endowed professorship (to F.J.C.).

* To whom to address correspondence.
‡ Michigan State University.
§ University of Notre Dame.

⊗ Abstract published in *Advance ACS Abstracts,* February 1, 1996.

[1] Abbreviations: Pg, human plasminogen; Pm, human plasmin; tPA, tissue-type plasminogen activator; UK, urokinase-type plasminogen activator; $K1_{Pg}$, $K2_{Pg}$, $K3_{Pg}$, $K4_{Pg}$, and $K5_{Pg}$, the kringle 1−kringle 5 domains of human plasminogen consisting of amino acid residues Cys84−Cys162, Cys166−Cys243, Cys256−Cys333, Cys358−Cys435, and Cys462−Cys541, respectively; $K2_{tPA}$, the kringle 2 domain of tissue-type plasminogen activator consisting of residues Cys180−Cys261; EACA, ϵ-aminocaproic acid; AMCHA, *trans*-(aminomethyl)-cyclohexanecarboxylic acid.

0006-2960/96/0435-2567$12.00/0

also dependent upon carboxy-terminal lysine residues and perhaps other internal lysine or pseudo-lysine residues (Varadi & Patthy, 1983, 1984). In all of these cases, binding of Pg is inhibited by ω-amino acids. Interactions of Pg with a variety of cells have also been reported, and it was found that a region of the Pg molecule comprising its first three kringle domains serves as the primary cellular binding locus (Miles et al., 1988). The ω-amino acids also displace Pg in this binding interaction.

The role of kringle domains in binding events such as these and the ability of ω-amino acid ligands to displace Pg from physiological regulators have stimulated a large number of investigations aimed at identifying the physical and chemical characteristics of the binding sites for these small molecule ligands to isolated kringle domains. The strongest ω-amino acid binding site on Pg is contained within its $K1_{Pg}$ module (Lerch & Rickli, 1980; Menhart et al., 1991), with weaker sites present on $K2_{Pg}$ (Marti et al., 1994), $K4_{Pg}$ (Lerch & Rickli, 1980; De Marco et al., 1987; Sehl & Castellino, 1990; McCance et al., 1994), and $K5_{Pg}$ (Novokhatny et al., 1989; Thewes et al., 1990; McCance et al. ,1994). While some of the amino acids involved in stabilizing interactions of $K1_{Pg}$ with ω-amino acid ligands have been derived from results of site-directed mutagenesis studies, a more rational approach to additional mutagenesis experiments and the interpretation of such work would accrue most with the consideration of crystal structures of the complexes. Comparison of the complexes of $K1_{Pg}$/EACA and $K1_{Pg}$/AMCHA with each other and with apo-$K1_{Pg}$ would, in addition, allow proposals to be formulated and tested with respect to the molecular basis of the much tighter binding observed for AMCHA in relation to EACA. We thus believed it relevant to obtain the X-ray crystal structures of the $K1_{Pg}$/EACA and $K1_{Pg}$/AMCHA complexes and compare them with that of apo-$K1_{Pg}$. These ligand/kringle structures are provided and described herein while that for apo-$K1_{Pg}$ was determined earlier (Wu et al., 1994).

MATERIALS AND METHODS

Expression and Purification of $K1_{Pg}$. The cDNA encoding the $K1_{Pg}$ module of Pg was constructed, expressed in *Escherichia coli*, and purified according to our previously published methodology (Menhart et al., 1991).

Crystallization. Human $K1_{Pg}$ was used as a lyophilized powder stored at freezer temperatures. A 25 mM stock solution of EACA (Aldrich Chemical Co., Milwaukee, WI) was prepared in deionized filtered water, and a 10-fold excess of this agent was added to $K1_{Pg}$, similarly dissolved. The final $K1_{Pg}$ concentration was 10.3 mg/mL.

Incomplete factorial searches (Carter & Carter, 1979; Jancarik & Kim, 1991; Cudney et al., 1994) using the hanging drop method were carried out to optimize crystallization conditions for the $K1_{Pg}$/EACA complex. The reservoir contained 1 mL of the factorial solution, and the hanging drops consisted of 2 μL of the protein solution added to 2 μL of the reservoir solution. Crystals (0.3 mm $\times$ 0.2 mm $\times$ 0.1 mm) grew in *ca*. 6 weeks as thin plates and long rectangular prisms from 1.6 M sodium citrate, pH 6.5.

Crystallizations with $K1_{Pg}$ and AMCHA (Sigma Chemical Co., St. Louis, MO) were conducted as with EACA and occurred from a solution of 1.4−1.5 M sodium citrate, pH 6.5, as small thin plates in *ca*. 2 days. One of these crystals was macroseeded in a drop with 1.6 M citric acid adjusted to pH 6.5 with LiOH. Multiple macroseeding produced a crystal of dimensions 0.4 mm $\times$ 0.25 mm $\times$ 0.02 mm.

Table 1: R-AXIS Intensity Data Statistics of $K1_{Pg}$ Complexes

	shell			cumulative	
resolution (Å)	$\langle\|F_o\|^2/\sigma\rangle$	obsd (%)	R_{merge} (%)	obsd	%
$K1_{Pg}$/EACA					
10.00	13.6	83.3	5.5	90	83.3
5.00	14.1	91.7	5.5	686	90.5
3.00	12.2	95.0	6.4	3122	94.0
2.50	7.9	95.0	9.4	5313	94.4
2.06	5.3	93.4	12.8	9309	93.9
$K1_{Pg}$/AMCHA					
10.00	11.6	70.0	5.7	84	70.0
5.00	11.8	83.3	5.6	648	81.3
3.00	8.9	82.9	6.6	2820	82.5
2.50	5.3	69.9	10.2	4472	77.4
2.07	3.8	60.0	13.3	7028	70.0

Intensity Data Collection. X-ray diffraction intensity data collection was carried out with a R-AXIS II imaging plate detector using 0.3 mm collimated graphite monochromated Cu Kα radiation from a Rigaku RU200 rotating anode generator operating at 5 kW power with a fine focus filament (0.3 mm $\times$ 0.3 mm). The crystal−plate distance was 100 mm, and each frame was collected for 45 min with an oscillation range of 3.0° for $K1_{Pg}$/EACA and for 90 min in a 2.5° range for $K1_{Pg}$/AMCHA. The unit cells were determined by autoindexing: $K1_{Pg}$/EACA, monoclinic, a = 34.52 Å, b = 51.61 Å, c = 46.54 Å, β = 111.7°, space group $P2_1$, 4 molecules/unit cell (2 per asymmetric unit); $K1_{Pg}$/AMCHA, orthorhombic, a = 64.33 Å, b = 51.69 Å, c = 46.77 Å, space group $P2_12_12_1$; 8 molecules/unit cell (2 per asymmetric unit). Processing of the raw data was conducted with the Rigaku R-AXIS processing software package. A total of 39 205 observations with $|F| > 1.0\sigma$ were made on $K1_{Pg}$/EACA, of which 9309 were unique reflections (2.06 Å resolution, R_{merge} = 7.63%, 93.9% completion), and a total of 17 924 observations were made for $K1_{Pg}$/AMCHA, of which 7028 were unique (2.07 Å resolution, R_{merge} = 7.95%, 70% completion). A more detailed summary of the intensity data collections is given in Table 1.

Structure Determination. Both structures were solved using molecular replacement rotation/translation methods. The coordinates of apo-$K1_{Pg}$ (Wu et al., 1994) were used as a search model. The searches were carried out with the program X-PLOR (Brunger, 1990) for $K1_{Pg}$/EACA and AMoRe (Navaza, 1994) for $K1_{Pg}$/AMCHA. A self-rotation function was calculated with $K1_{Pg}$/EACA to fix the noncrystallographic symmetry relating the independent kringle molecules. The highest peak was 8.6σ (6.8σ above the mean), and the angles corresponded to a noncrystallographic 2-fold rotation axis approximately parallel to the *a*-axis. The two highest solutions of the cross-rotation search had peak heights 5.1σ and 4.6σ, and the rotation matrices of individual molecules were in agreement with the self-rotation matrix. The translation search with these rotation solutions gave peak heights of 15.4σ and 16.6σ for the two solutions (correlation coefficients were 0.31 and 0.30, respectively). The relative *y*-translation between kringle molecules 1 and 2 was determined by a combined translation function search. A rigid body refinement with both molecules gave an *R*-value of 38.9%. This model was then used for a positional refinement, which reduced the *R*-factor to 26.6%.

Table 2: Target Refinement Parameters and RMS Deviations

property	target	EACA	AMCHA
distances			
bond distance (Å)	0.02	0.02	0.02
angle distance (Å)	0.04	0.05	0.05
planar 1,4-distance (Å)	0.06	0.06	0.06
miscellaneous			
planar groups (Å)	0.04	0.04	0.03
chiral centers (Å^3)	0.15	0.19	0.18
nonbonded distance			
single torsion (Å)	0.60	0.23	0.23
multiple torison (Å)	0.60	0.28	0.32
possible H-bond (Å)	0.60	0.32	0.28
noncrystallographic symmetry			
main chain (Å)	0.50	0.21	0.23
side chain (Å)	1.00	0.43	0.49
thermal restraints			
main-chain bond (Å^2)	1.5	1.2	1.0
main-chain angle (Å^2)	2.0	1.7	1.4
side-chain bond (Å^2)	2.5	2.5	2.0
side-chain angle (Å^2)	3.0	3.1	2.6
RMS bond angle (deg)		3	3
atoms/asymmetric unit		1444	1450
water molecules		148	150
R-factor (%)		16.8	17.8
diffraction pattern: $\sigma(\|F_o\|) = A + B(\sin\theta)/\lambda - {}^1/_6)$			
$\langle\Delta F\rangle$		22	38
A		13.5	21.0
B		−80	−75

The molecular replacement calculations for $K1_{Pg}$/AMCHA were carried out using the AMoRe program package. The rotational search provided two outstanding solutions with a correlation coefficient of 0.27. The translation search using both of these solutions gave a final *R*-value of 29.9%, with a correlation coefficient of 0.82. Further refinement was carried out with the X-PLOR program package using data in the resolution range 9.0−3.0 Å. The positional refinement of this model reduced the *R*-factor to 27.2%.

Structure Refinement. The refinement of the structures was carried out using the programs PROLSQ (Hendrickson, 1985) and PROFFT (Finzel, 1987). After 18 cycles, the refinement converged to an *R*-value of 21.5% for $K1_{Pg}$/EACA and 21.1% for $K1_{Pg}$/AMCHA. The electron and density difference maps clearly indicated the presence of the ligands in the ω-amino acid binding sites. Further refinement proceeded including the ligands in the calculations. The $K1_{Pg}$/EACA structure, refined with and without noncrystallographic symmetry restraints, yielded similar results. Since the diffraction data were only of average quality, restraining the symmetry is advantageous (Tulinsky & Blevins, 1986), and this strategy was followed herein. Solvent water molecules were located and added periodically in refinement beyond 2.5 Å resolution by examining the $(|F_o| - |F_c|)$ maps in two different resolution ranges: 9.0−2.5 and 7.5−2.5 Å. Larger peaks common to both and also in the $(2|F_o| - |F_c|)$ map that were within 4.0 Å of protein atoms were usually selected as water molecules. The final structure of the $K1_{Pg}$/EACA complex converged at a *R*-factor of 0.168 using 148 water molecules with occupancies >0.5 and 8641 reflections. The final $K1_{Pg}$/AMCHA structure converged at 0.178 with 150 water molecules and 5900 reflections. Only Glu47 had outlier ϕ, ψ angles, similar to that of apo-$K1_{Pg}$ (Wu et al., 1994) and Met48 of $K4_{Pg}$ (Mulichak et al., 1991). A summary of the refinement statistics is given in Table 2.

The coordinates of both structures have been deposited in the Brookhaven Protein Data Bank: $K1_{Pg}$/EACA (1CEA) and $K1_{Pg}$/AMCHA (1CEB).

RESULTS

Although the $K1_{Pg}$/EACA and $K1_{Pg}$/AMCHA complexes crystallize in different crystal systems, the local packing arrangements of the two are very similar. Both possess a crystallographic 2_1 screw axis along the *y*-direction, but $K1_{Pg}$/AMCHA had, in addition, two other mutually perpendicular screw axes. The local noncrystallographic 2-fold rotation axis of the monoclinic $K1_{Pg}$/EACA crystals (along the *x*-direction for both structures), however, also gives rise to local 2_1 screw axes so that the packing in the monoclinic form is pseudo $P2_12_12_1$ and resembles the orthorhombic crystals of K1Pg/AMCHA. The relationship between the $K1_{Pg}$ molecules in the two unit cells is an anticlockwise 21° rotation of the monoclinic structure accompanied by translations $x = -6.3$ Å, $y = -38.8$ Å, and $z = -3.5$ Å (the large difference in *y* is due to the arbitrary nature of the origin along *y* in space group $P2_1$). Thus, it has been possible to identify the same local 2-fold rotation *dimer* in the asymmetric unit of the two different crystals. The immediate packing arrangement around a dimer is the same in both structures, but the similarity deteriorates at long range because two of the screw axes in the monoclinic crystals are not crystallographic.

Both of the kringle complexes contain two molecules in the asymmetric unit of the crystal structure (Figure 1), similar to $K4_{Pg}$ in crystals of the monoclinic form of this particular kringle (Padmanabhan et al., 1994). Nearly all of the $K1_{Pg}$ structure is well-defined in the electron density in both complexes. The most notable exception is the side chain of the cationic center of Arg34[2] in the ω-amino acid binding site. In this case, the density extends to NE in molecule 1 of the $K1_{Pg}$/AMCHA complex, a situation similar to that found in the apo-$K1_{Pg}$ (Wu et al., 1994). Electron density only to CB was observed in molecules 1 and 2 of the EACA and AMCHA complexes, respectively, but the residue has full density in molecule 2 of $K1_{Pg}$/EACA. All of this is difficult to reconcile completely considering the immediate packing arrangement in both dimers is essentially the same. The different Cα−kringle structures of the complexes have been compared with each other in Table 3, and the data therein indicate that they are the same within the expected error of the independent determinations. Although the differences are somewhat larger, the same essentially applies when the comparison is extended to the apo-$K1_{Pg}$ (Table 3), even though apo-$K1_{Pg}$ has different crystal contacts than the complexes. The two kringles in the $K1_{Pg}$/EACA and $K1_{Pg}$/AMCHA complexes have RMSΔ values of 0.37−0.38 Å. From the values in Table 3, it appears that molecule 2 of $K1_{Pg}$/EACA may be slightly different from the other three.

Computer-generated distances between the ligands and charged and polar amino acid side-chain residues in the $K1_{Pg}$ binding pockets have been obtained in order to identify those that potentially stabilize ligand binding. The results for each of the component molecules of both dimers are provided in Table 4 and illustrated in Figure 2 for $K1_{Pg}$/EACA and Figure 3 for $K1_{Pg}$/AMCHA (see Figure 4 for the manner in which the atoms of EACA and AMCHA have been labeled). These data reveal that the major ionic and/or polar contributors to the ligand binding energy are most likely Asp54, Asp56,

[2] All residue numbering in kringles begins with the first Cys residue of the kringle and proceeds sequentially (without gaps) to the last Cys residue.

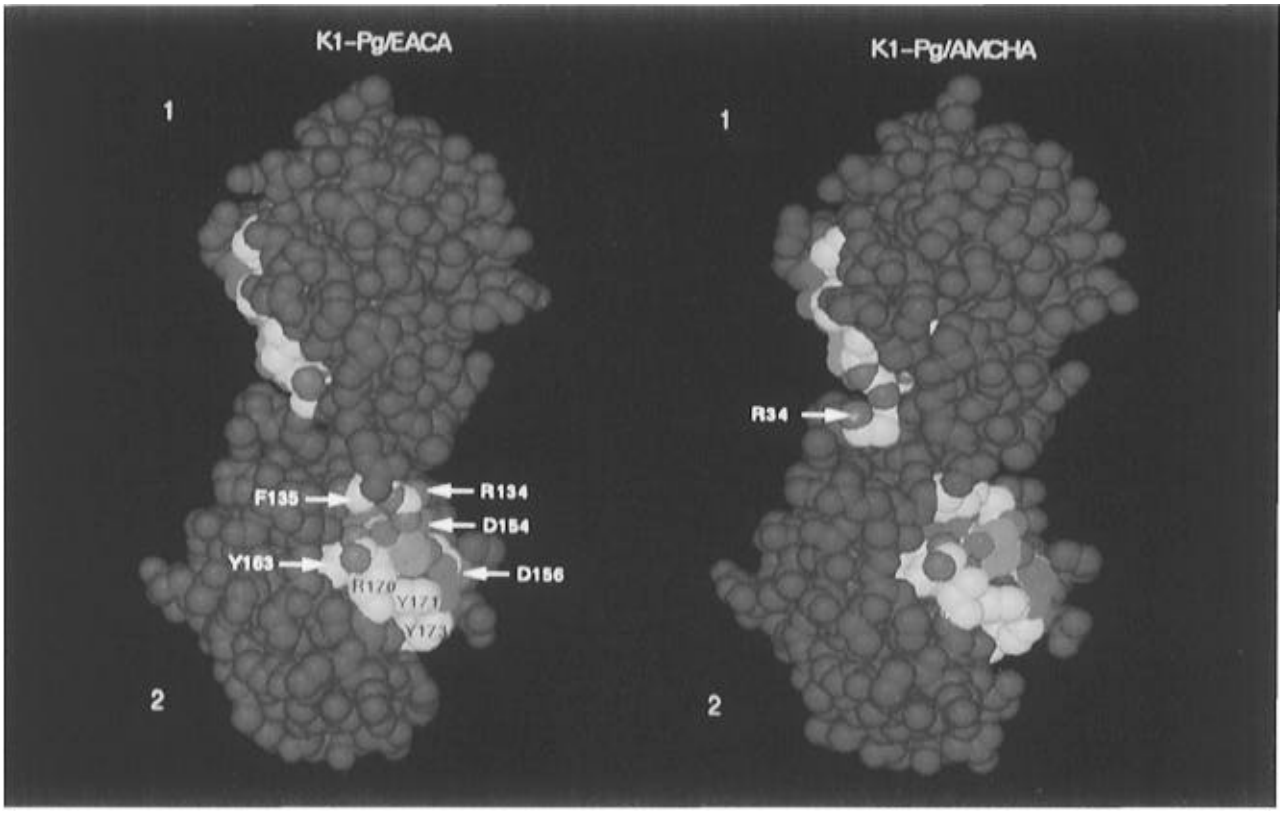

FIGURE 1: Space-filling representations of the structures of the $K1_{Pg}$/EACA and $K1_{Pg}$/AMCHA dimers. The carbon atoms of the ligands in the binding pockets are highlighted (green), as are most side chains of amino acid residues (in orange) implicated in direct ligand−kringle interactions. Trp61 is not visible in these views. All other amino acids of the kringle are colored dark red. In all cases, nitrogen atoms of the highlighted regions are dark blue and oxygen atoms red. Orientations correspond to backbone atoms (C, CA, N, O) of the $K1_{Pg}$/ligand complexes superimposed on each other in three-dimensional space. $K1_{Pg}$ amino acid residues are numbered 1−79 and 101−179 in molecules 1 and 2, respectively, of the dimers.

Table 3: RMSΔ (Å) between CA Structures of Independent Kringles

molecule	EACA-1	EACA-2	AMCHA-1	AMCHA-2
AMCHA-2	0.29	0.42	0.37	
EACA-1		0.38	0.30	
EACA-2			0.42	
apo-$K1_{Pg}$	0.57	0.55	0.57	0.61

Table 4: Ion Pair and Hydrogen-Bonding Interactions of EACA and AMCHA in the Ligand Binding Site[a]

EACA	residue	1[b]	2[b]	AMCHA	1[b]	2[b]
O1	Arg34-NH1		2.43			
NZ	Asp54-OD1	3.01	2.69	N	2.82	2.65
NZ	Asp56-OD1	2.99	2.51	N	3.05	2.88
O2	Tyr63-OH	2.60	2.31	O2	2.51	2.41
O1	Arg70-NE	3.05	3.04	O1		2.77
O1	Arg70-NH1		3.15			
	Arg70-NH2			O1	2.69	3.04
	Arg70-NH2			O2		3.01

[a] Distances of <3.2 Å are listed. [b] Molecules 1 and 2 of each complex in the crystal unit cell.

Tyr63, Arg70, and possibly Arg34. Other amino acids that potentially make side-chain contacts with the ligands through van der Waals forces have been identified in the crystal structures by assuming that such contacts would be of importance when distances between atoms are ≤4 Å. These atoms are listed in Table 5 and show that the principal direct contributions are from the side chains of amino acids Trp61, Tyr63, and Tyr71, with a smaller contribution from Phe35. Each of these amino acids possesses interatomic distance relationships with the ligands suggestive of multiple van der Waals contacts of the kringle binding site with atoms within the ligands.

Another method used to reveal the comparative nature of binding of EACA and AMCHA to $K1_{Pg}$ was by evaluation of the accessible area of the ligand binding site of the complexes. The accessible area was calculated as that which contacts a sphere of 1.4 Å radius as it migrates around the surface (Lee & Richards, 1971) of the ω-amino acid site. The binding site region used was that defined previously, *viz.*, His31−Phe35, Pro53−Pro57, Pro60−Tyr63, and Arg70−Cys74 (Tulinsky et al., 1988). The values obtained for uncomplexed $K1_{Pg}$ and for each molecule of the complexes of EACA and AMCHA of the unit cell are provided in Table 6.

DISCUSSION

On the basis of analyses of a variety of isolated kringle domains by chemical modification (Lerch & Rickli, 1980; Trexler et al., 1982, 1985; Vali & Patthy, 1984), NMR spectroscopy (Llinas et al., 1985; Trexler et al., 1985; De Marco et al., 1986, 1989; Petros et al., 1989; Thewes et al., 1990), molecular modeling (Tulinsky et al., 1988), X-ray crystallography (de Vos et al., 1992; Mulichak et al., 1991; Wu et al., 1991, 1994), and site-directed mutagenesis (De Serrano & Castellino, 1992a,b, 1993; Hoover et al., 1993; McCance et al., 1994), a general concensus regarding the minimal number of amino acid residues needed for direct stabilization of ω-amino acids to several kringle domains has been developed. In this binding pocket, Asp54 and Asp56 of the kringle stabilize the amino group of the ligand

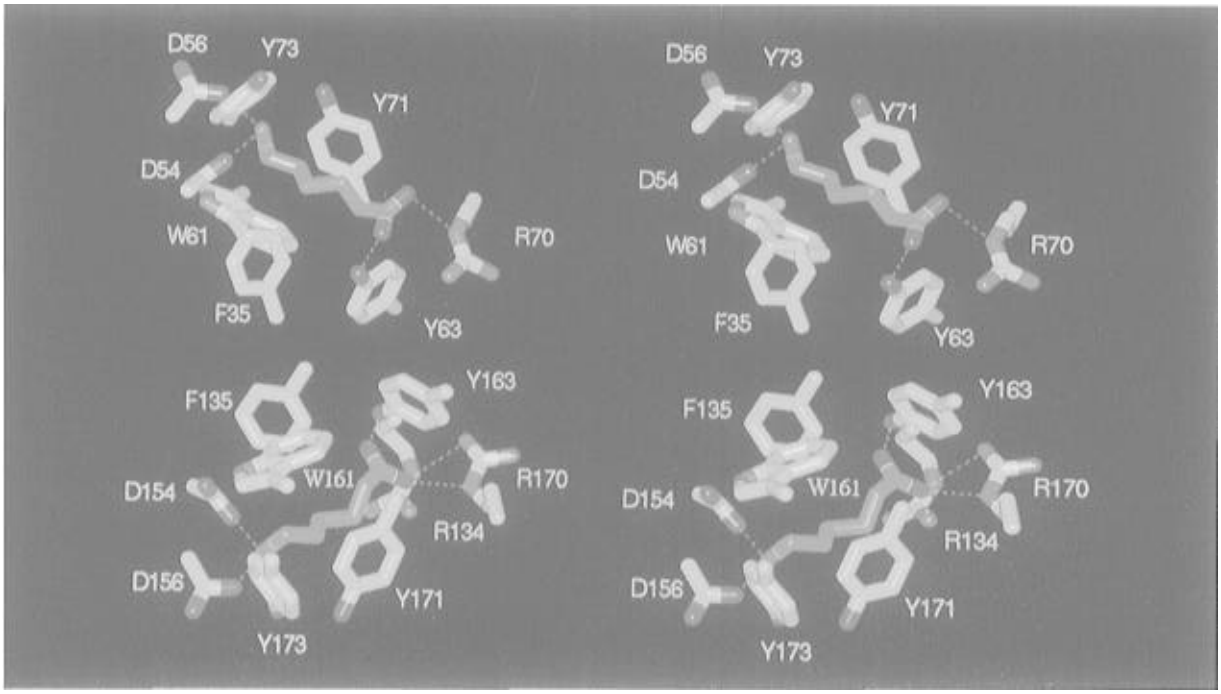

FIGURE 2: Stereoview of the relationships of EACA and specific amino acid side chains of $K1_{Pg}$. Molecules 1 and 2 of the dimeric complex are related by a local 2-fold rotation axis running left to right. The distance between molecules 1 and 2 is arbitrary (see Figure 1). The amino acid side-chain carbon atoms of the kringle are colored orange, and those of EACA are in green. For other atoms, blue represents nitrogens and oxygens are in red. The Arg34 side chain possessed electron density only to the CB group in molecule 1 of the dimer (not displayed) and full side-chain electron density in the corresponding molecule 2. The dotted green lines show the most probable electrostatic and hydrogen-bonding interactions of EACA with these side-chain residues, as indicated from the distance measurements of Table 4. $K1_{Pg}$ amino acid residues are numbered 1−79 and 101−179 in molecules 1 and 2, respectively, of the dimers.

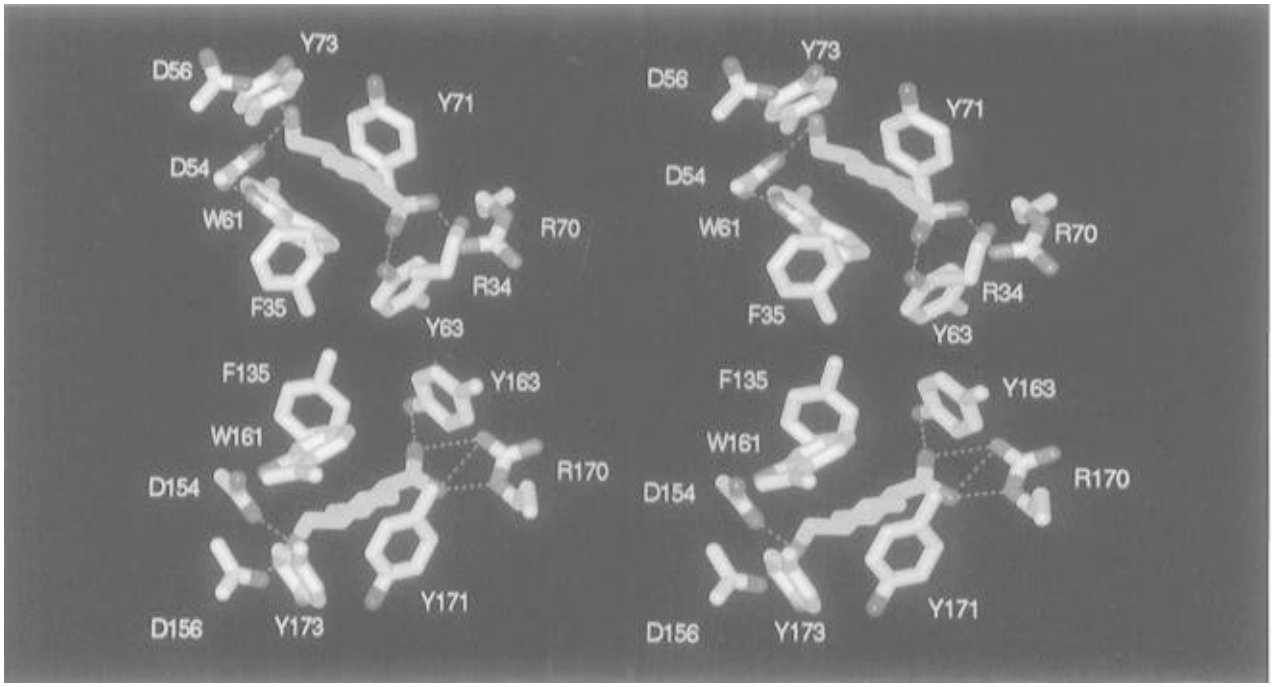

FIGURE 3: Stereoview of the relationships of AMCHA and amino acid side chains of $K1_{Pg}$. Molecules 1 and 2 of the dimeric complex are related by a local 2-fold rotation axis running left to right. The distance between molecules 1 and 2 is arbitrary (see Figure 1). The side-chain carbon atoms of the kringle are colored pink, and those of AMCHA are in yellow. For other atoms, dark blue represents nitrogen and oxygens are in red. The Arg34 side chain possessed electron density only to the NE group in molecule 1 of the dimer and only to CB in the corresponding molecule 2. Since these atoms of Arg34 are not involved in binding to the ligand, they are not displayed in the figure. The dotted green lines show the likely electrostatic and hydrogen-bonding interactions of AMCHA with these side-chain residues, as indicated from the distance measurements of Table 4. $K1_{Pg}$ amino acid residues are numbered 1−79 and 101−179 in molecules 1 and 2, respectively, of the dimers.

(Weening-Verhoeff et al., 1990; de Vos et al., 1992; Mulichak et al., 1991; Wu et al., 1991; De Serrano & Castellino, 1993; Hoover et al., 1993; McCance et al., 1994), and the carboxylate group of the ligand is stabilized by Lys33 in $K2_{tPa}$ (de Vos et al., 1992; De Serrano & Castellino, 1992a; De Serrano et al., 1992) and Arg69 or Arg70 (Mulichak et al., 1991; Hoover et al., 1993; Wu et al., 1991, 1994; McCance et al., 1994) and possibly a Lys or Arg residue in

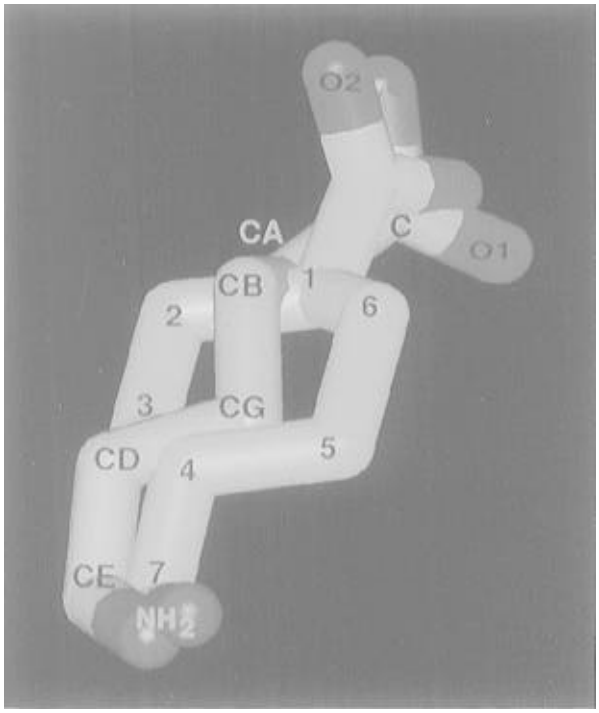

FIGURE 4: Conformations of EACA (orange carbon backbone) and AMCHA (light blue carbon backbone) in the binding site of $K1_{Pg}$ molecule 2 of the dimer. For other atoms, dark blue represents nitrogen and oxygens are in red. The atoms are numbered and lettered according to their listing in Tables 4 and 5 and are consistent with textual references to the carbon atoms of these ligands.

the vicinity of residue 35 (Mulichak et al., 1991), in plasminogen kringles. Several aromatic amino acid residues are perturbed as a result of ω-amino acid binding to kringles (Llinas et al., 1985; Trexler et al., 1985; De Marco et al., 1986, 1989; Petros et al., 1989; Thewes et al., 1990). The perturbation, however, is fairly small (Wu et al., 1991). Site-directed mutagenesis studies have implicated Trp74 of $K2_{tPA}$ (De Serrano & Castellino, 1992b) and the homologous Tyr71 in $K1_{Pg}$ (Hoover et al., 1993), Trp70 in $K4_{Pg}$ (McCance et al., 1994), and Tyr72 in $K5_{Pg}$ (McCance et al., 1994) to be of direct importance to stabilizing binding of ω-amino acids. This aromatic residue forms one wall of an aromatic trough that stabilizes the hydrophobic core of the ω-amino acid ligand, the other wall being formed by Trp61 of $K1_{Pg}$ (Wu et al., 1994) or the homologous aromatic residue found in that location in all other kringles that bind ω-amino acids, *viz.*, Trp63 in $K2_{tPA}$ (de Vos et al., 1992), Trp60 in $K4_{Pg}$ (Mulichak et al., 1991; Wu et al., 1991), and Trp62 in $K5_{Pg}$.

From the X-ray crystal structures obtained in this current investigation, we conclude that the ω-amino acid binding site of $K1_{Pg}$ for its ligands, EACA and AMCHA, is characterized by a dipolar surface, the extremities of which are separated by a V-shaped hydrophobic trough formed by the indole ring of Trp61 and the phenolic ring of Tyr71. These have perpendicular aromatic stacking interactions with the rings of Tyr63 and Tyr73, respectively, as illustrated in Figure 5 and 6, all of which form a stabilized structural framework for interacting with methylene or other nonpolar groups of ligands. The anionic center is at one end of the dipolar surface (Asp54, Asp56) and the cationic center (Arg34, Arg70) at the other end (Figures 2 and 3). However, the side chain of Arg34 is outside that of Arg70 in apo-$K1_{Pg}$ and present in the solvent region, probably due to like-charge repulsion (Wu et al., 1994). Mutagenesis experiments

Table 5: Ligand van der Waals Contacts (Å) with Aromatic Side-Chain Residues of $K1_{Pg}$ < 4.0 Å

CG	residue	1[a]	2[a]	AMCHA	residue	1[a]	2[a]
CG	Phe35-CH1	3.73		C1	Phe35-CE1		3.94
O2	Phe35-CD1		3.02	C6	Phe35-CE1		3.97
	Phe35-CE1		3.48	O2	Phe35-CD1	3.75	3.73
					Phe35-CE1		3.69
CA	Trp61-CH2		3.96	C3	Trp61-CE2	3.87	
CG	Trp61-CZ2	3.85			Trp61-CZ2	3.81	3.68
	Trp61-CH2	3.54			Trp61-CH2	3.81	3.34
	Trp61-CZ3	3.97			Trp61-CZ3	3.97	3.53
CD	Trp61-CE2	3.98		C4	Trp61-CZ2		3.98
	Trp61-CZ2	3.87		C7	Trp61-NE1	3.53	3.72
	Trp61-CH2	3.78			Trp61-CE2	3.90	3.31
	Trp61-CZ3	3.86			Trp61-CZ2		3.23
CE	Trp61-CD1		3.93		Trp61-CH2		3.87
	Trp61-NE1	3.75	3.61				
	Trp61-CD2	3.45	3.50				
	Trp61-CZ2	3.63	3.92				
	Trp61-CD2	3.83	3.74				
CA	Tyr63-CE1	3.36		C1	Tyr63-OH	3.84	3.86
	Tyr63-CZ	3.53	3.89	C8	Tyr63-CE1	3.98	3.85
	Tyr63-OH	2.99	3.32		Tyr63-CZ		4.00
C	Tyr63-CH1	3.67	3.71		Tyr63-OH	3.21	3.32
	Tyr63-CZ	3.89	3.60	O1	Tyr63-OH	3.81	
	Tyr63-OH	3.13	2.76	O2	Tyr63-CE1		3.55
O1	Tyr63-CE1		3.96		Tyr63-CZ	3.66	3.36
	Tyr63-OH		3.60		Tyr63-OH	2.51	2.40
O2	Tyr63-CE1	3.85					
	Tyr63-CZ	3.69	3.51				
	Tyr63-OH	2.60	3.31				
CD	Tyr71-CG		3.81	C2	Tyr71-CG	3.77	3.69
	Tyr71-CD1		3.91		Tyr71-CD1	3.50	3.59
	Tyr71-CE1		3.77		Tyr71-CE1	3.68	
	Tyr71-CZ	3.78	3.46	C3	Tyr71-CG	3.64	3.61
	Tyr71-CE2	3.72	3.39		Tyr71-CD1	3.79	3.87
	Tyr71-CD2	3.92	3.53		Tyr71-CE1	3.85	
CE	Tyr71-CE2	3.98	3.60		Tyr71-CZ	3.74	
	Tyr71-CD2		3.86		Tyr71-CE2	3.71	3.83
					Tyr71-CD2	3.69	3.60

[a] Molecules 1 and 2 in the crystal unit cell.

Table 6: Accessible Areas of EACA and AMCHA and the Ligand Binding Site

complex	LBS[a] + ligand (Å^2)	ligand in complex (Å^2)	total ligand (Å^2)	% ligand exposed
$K1_{Pg}$	919[a,b]			
$K1_{Pg}$/EACA-1	868[a]	74	333	22
$K1_{Pg}$/EACA-2	848[a]	64	333	19
$K1_{Pg}$/AMCHA-1	904[a]	81	344	24
$K1_{Pg}$/AMCHA-2	860[a]	78	344	23

[a] Accessibility of the complete kringle complex was calculated first. Values listed are the sum of ω-amino acid binding site components only to the total accessibility. [b] No ligand present (Wu et al., 1994).

show clearly that replacement of Arg34 with Gln does not affect the K_d values that characterize binding of EACA and AMCHA to $K1_{Pg}$ (Hoover et al., 1993). A similar result has been reported for $K4_{Pg}$ (Nielsen et al., 1993; McCance et al., 1994), thus excluding Lys35 as a significant factor in $K4_{Pg}$−ligand interactions in solution and confirming that in this case Arg69 functions solely as the cationic site (McCance et al., 1994). The participation of Lys35, however, is undeniable in the crystal structure of the $K4_{Pg}$/EACA complex (Wu et al., 1991), suggesting that small differences exist between the crystal and solution structures of this complex. Additional mutagenesis investigations show that in the $K2_{tPA}$/EACA complex the only cationic locus of the kringle that coordinates the carboxylate of the ligand is Lys33

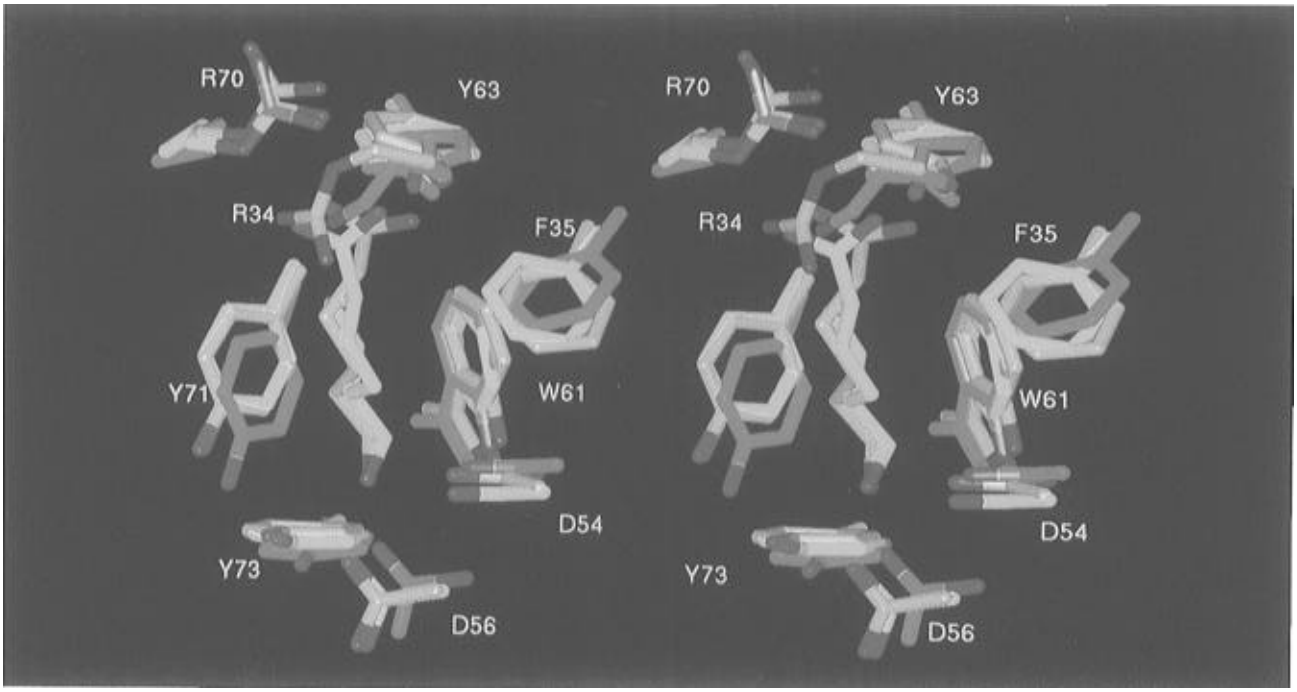

FIGURE 5: Stereoview of the relationships of critical amino acid side-chain residues in the $K1_{Pg}$/ligand complexes and of apo-$K1_{Pg}$. In this illustration, the backbone atoms (C, CA, N, O) of the peptide chains of apo-$K1_{Pg}$ and the two $K1_{Pg}$/ligand complexes are superimposed on one another in three-dimensional space. In the cases of the $K1_{Pg}$/ligand complexes, molecule 2 of the dimer is used as the example. The side-chain carbon atoms of apo-K1 are colored green, and those of $K1_{Pg}$/EACA and $K1_{Pg}$/AMCHA are in orange and light blue, respectively. For other atoms, dark blue represents nitrogens and oxygens are in red. The crystal coordinates used for apo-$K1_{Pg}$ have been taken from published work (Wu et al., 1994). This illustration emphasizes the movement of the side chains of several residues upon ligand complexation and the perpendicular stacking of the rings of Trp61 and Tyr63, as well as those of Tyr71 and Tyr73. The amino acid side-chain residues that are displayed are numbered according to their location in apo-$K1_{Pg}$.

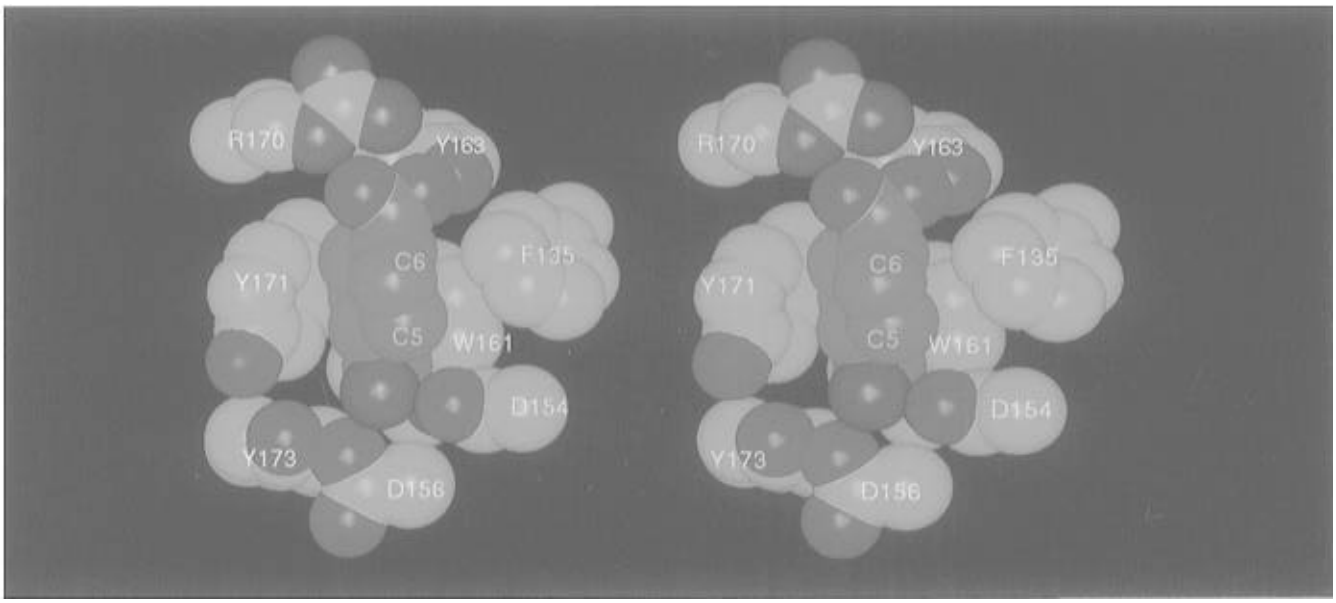

FIGURE 6: Stereoview of the relationships of AMCHA and amino acid side chains in the binding pocket of $K1_{Pg}$/AMCHA molecule 2. The carbon atoms of AMCHA are colored green, and those of $K1_{Pg}$ amino acid side chains are in blue. For other atoms, blue represents nitrogens and oxygens are in red. The C5 and C6 carbon atoms of AMCHA are labeled. For Arg134, electron density only to CB was observed (not displayed). $K1_{Pg}$ amino acid residues are numbered 101−179 in reference to molecule 2 of the dimer.

(De Serrano & Castellino, 1992a; De Serrano et al., 1992). This is in agreement with conclusions from the crystal structure of $K2_{tPA}$, which is a lysine pseudo-ligand intermolecular complex that clearly suggests Lys33 in this role and eliminates the possible involvement of the Lys68−Arg70−Arg71 cluster in stabilization of ligand binding (de Vos et al., 1992). The latter contention has also been confirmed by results of site-directed mutagenesis studies (De Serrano & Castellino, 1992a; De Serrano et al., 1992).

In the $K1_{Pg}$/EACA complex, the ligand lies between the charged centers of the ω-amino acid binding site of the kringle in an extended conformation (Figures 2 and 4). Binding at the anionic center of both molecules of the dimer is the same: a doubly hydrogen bonded salt bridge between the amino group of EACA and Asp54/Asp56 (Table 4 and Figure 2). The interactions are necessarily different at the cationic center in the two $K1_{Pg}$ molecules because the structures differ (no density beyond CB of Arg34, molecule

1; full density in molecule 2). The EACA−kringle interactions common to both molecules 1 and 2 are hydrogen bonds between carboxylate oxygen O1 of EACA and Arg70-NE and between O2 of EACA and Tyr63-OH. From the orientation of the guanidinium group of Arg70 (Figure 2), this former interaction appears to be a lone hydrogen bond with little or no salt bridge component. In molecule 2, the ion pair interaction is stronger because the carboxylate of EACA is somewhat closer to Arg70 with a slightly different orientation that additionally leads to hydrogen bonds with Arg70-NH1 and Arg34-NH1. The new opportunity for Arg34 to also bind may be the reason that this Arg residue has full electron density in molecule 2. It thus appears that some differences exist in the binding of EACA to each molecule of $K1_{Pg}$, with increased ionic/hydrogen bonding occurring in molecule 2 of the dimeric complex (Table 4 and Figure 2).

The position of the amino group of AMCHA in $K1_{Pg}$/AMCHA is practically the same as that of EACA so the hydrogen-bonding salt bridge interactions are also similar (Table 4 and Figure 3). The cyclohexyl ring of AMCHA in the $K1_{Pg}$/AMCHA complex exists in a chair conformation (Figures 3 and 4). In both molecules 1 and 2 of the complex, binding of the carboxylate oxygen O1 of the ligand to $K1_{Pg}$ involves a hydrogen-bonded salt bridge with O1 of the carboxylate and Arg70-NH2 and a hydrogen bond with Tyr63-OH. The carboxylate of AMCHA in molecule 2, like EACA in molecule 2, is also closer to Arg70, thus forming a second hydrogen-bonded salt bridge, that between O2 of the carboxylate of AMCHA and Arg70-NH2, as well as a hydrogen bond between the O1 atom of the carboxylate and Arg70-NE. The hydrogen-bonded salt bridge interactions of AMCHA in the binding pocket of molecule 2 of the $K1_{Pg}$/AMCHA complex are subtly different from those same interactions in molecule 1 of the complex. In particular, the ligand/kringle binding energy is predicted to possess two additional stabilizing forces in molecule 2 and a slight change in orientation of the side chain of Asp56 (Figure 3). This is probably due to asymmetrical kringle−kringle interactions in the dimer, which lead to small changes in the geometry of the binding pocket.

An unanticipated result surfaced in the comparison of the van der Waals interactions of EACA and AMCHA with $K1_{Pg}$. In the past, it was assumed that AMCHA interacted more tightly with $K1_{Pg}$ [K_d(AMCHA) $\approx$ 1 μM, K_d(EACA) $\approx$ 11 μM] (Menhart et al., 1991) due to the expectation that the bulky cyclohexyl ring contributed more interactions than EACA within the ligand binding site. However, Table 5 clearly indicates that EACA and AMCHA possess nearly the same number of interactions with $K1_{Pg}$ residues in the binding pocket at distances <4.0 Å. Since the binding of both ligands is not identical in the two molecules of each complex (Tables 4 and 5), a degree of flexibility appears to be associated with ligand binding. This proves to be the result of minor differences in conformations of the ligand and the lysine binding site. The superimposition of the EACA positions on those of AMCHA (Figures 4 and 5) reveals that the conformation of EACA mimics the chair conformation of AMCHA and extends along the long axis of AMCHA, through the center of the cyclohexane ring. Bound AMCHA, therefore, appears to be rotated around the same axis of EACA, the net effect of which is that contacts of atoms C5 and C6 of AMCHA with Trp61 and Tyr71 are practically nonexistent (Figure 6 provides a view of the complex that particularly emphasizes this point), while atoms C2 and C3 of the ring appear to be more deeply positioned in the binding pocket than those equivalent atoms, CB and CG, of EACA. Consequently, the two extra atoms of AMCHA contribute little to the binding of the ligand to $K1_{Pg}$, and the distance calculations presented in Table 5 do not contain interactions of atoms C5 and C6 of AMCHA with Trp61 and Tyr71. The close alignment of EACA and AMCHA in the binding pocket is further emphasized by distances between the N and O2 atoms of the bound ligands (7.4 and 7.3 Å, respectively, in molecule 2). The N and O1 atoms of these ligands in molecule 1 are at slightly more variance (7.8 and 7.2 Å, respectively). The latter difference, however, can be strictly accounted for by the free bond rotation of the carboxylate of EACA to maximize a contact with Arg34-NH1. Considering that EACA and AMCHA have only 9 and 11 atoms, respectively, excluding protons, the nature of their interactions within the binding site are highly notable, with approximately 50 total contacts at distances <4.0 Å.

The amino group of the ligands is closely superimposed in all four structures, but a similar situation does not exist at the carboxylate moiety of the ligand, where conformations differ by small free bond rotations (Figure 5). The latter are most likely intimately involved with the exact nature of the cationic center interactions, which differ in the structures (Table 4 and Figures 2 and 3). The lack of precision in placement of the carboxylate group of the ligand in the binding pocket suggests that the carboxylate might not play as important a role in the binding process as other ligand−kringle interatomic interactions. This is in agreement with the fact that agents, such as pentylamine and hexylamine, still retain binding, albeit reduced in strength, to at least one kringle domain, $K5_{Pg}$ (Novokhatny et al., 1989), and the observation that the binding energy of dihexylamine to a mutant form of $K2_{tPA}$ in which the cationic binding center is altered to one that is anionic, *viz*., Lys33Glu−$K2_{tPA}$, is even greater than that of EACA to wild-type $K2_{tPA}$ (De Serrano & Castellino, 1992a).

The equivalence of binding geometry of EACA and AMCHA is also borne out by a comparison of the accessible area of the ligand binding site of the complexes (Table 6). As expected, the complexed ligand binding site possesses approximately the same accessible area in all four molecules (Table 6). The larger area of the unliganded site ($K1_{Pg}$) indicates that more atoms at the site are accessible to a molecule like water. The fact that the accessible area of the bound ligand (column 2) is only slightly larger for AMCHA than EACA agrees with the presence of the two additional atoms present in AMCHA, as compared to EACA. The marginally larger accessible area of the whole AMCHA molecule (column 3) is again in agreement with the inaccessibility of the center of the ring, or the inner side of the ring atoms, to the 1.4 Å radius probe atom. The two additional atoms in AMCHA, as compared to EACA, nearly compensate for the effect. Lastly, the amount of bound ligand exposed to solvent in each case is also very similar, at approximately 20%. The foregoing indicate that there is very little difference in the bound states of the ligands and ω-amino acid binding site because the AMCHA ligand inserts in an edgewise fashion into the binding site (Figure 6), and few, or similar, conformational changes occur in the kringle upon binding of each of the ligands.

The equivalency of geometry of binding of EACA and AMCHA raises the question of reasons for the tighter binding of AMCHA to $K1_{Pg}$, relative to that of EACA. Some bearing on the question occurs from consideration of a previous investigation of the values of the individual rate constants involved in determining the binding equilibrium constants to $K4_{Pg}$ (De Marco et al., 1987). In this system, it was shown that the k_{on} for AMCHA is 2-fold greater than that for EACA, while the k_{off} for AMCHA is approximately 4-fold smaller. This accounts for an approximate 8-fold stronger binding energy of AMCHA, as compared to EACA. The faster k_{on} for AMCHA can be rationalized somewhat by its edgewise insertion into the binding pocket. The lower constraints for AMCHA binding may allow a greater number of $K1_{Pg}$ surface conformations to be favorable for binding, as opposed to EACA, which must more completely insert into the binding pocket. In addition is the fact that the conformation of AMCHA is much more fixed than that of EACA, and a relatively larger percentage of the total conformational pool of AMCHA molecules would be favorable for binding. Molecular collisions, therefore, should be more productive for AMCHA, as compared to EACA, and this would lead to a larger value for k_{on}. With regard to the lower k_{off} of AMCHA, it is possible that the hydrophobic solvent-exposed carbon atoms, *viz*., C5 and C6, of AMCHA are solvated in the complex by ordered water structures. The relative difficulty of disrupting this ordered water could result in enhancement of the entrapped AMCHA in the binding pocket, thus retarding k_{off}. Entropic factors may also be involved herein because EACA would be expected to have a larger decrease in entropy than AMCHA in the binding process.

Comparison of the binding site regions of the $K1_{Pg}$/EACA and $K1_{Pg}$/AMCHA complexes with apo-$K1_{Pg}$ reveals several small structural changes. The most noteworthy include displacements in the positions of Tyr63, Tyr71, and Tyr73 (the OH groups of each of these Tyr in the $K1_{Pg}$/EACA and $K1_{Pg}$/AMCHA complexes are displaced by 0.7−1.0 Å from that of apo-$K1_{Pg}$) and a reorientation of the ring of Phe35, the latter approaching 90° (Figure 5). These changes are observed in all of the four independent kringles of the complexes and appear to support binding by adjusting the region to a more compact state in the presence of the ligand. Additionally, the guanidinium group of the cationic center has a somewhat different orientation in three of the four liganded complexes (see Figure 5 for an example with molecule 2 of the $K1_{Pg}$/ligand complexes) and is nearly the same as apo-$K1_{Pg}$ only in molecule 1 of the AMCHA complex. A more significant repositioning (by >0.5 Å) of the guanidino group is found for the $K1_{Pg}$/EACA complex than for the $K1_{Pg}$/AMCHA complex. Each of the side-chain carboxylates of both Asp54 and Asp56 in both the $K1_{Pg}$/EACA and $K1_{Pg}$/AMCHA complexes are realigned somewhat upon substrate binding, with the changes more pronounced for Asp56 than for Asp54. Overall, however, while some degree of conformational adjustments are necessary to accommodate the ligands in an optimal fashion, those in the binding site are relatively small, and the site can be considered basically preformed and poised for binding for either of the ligands.

The solution structure of the $K1_{Pg}$/EACA complex was previously studied by NMR spectrometry (Rejante & Llinas, 1994). Although the NOE data were collected for the kringle in the presence of this ligand, only the $K1_{Pg}$ structure was computed, and EACA was not explicitly included. The structure of the complex was then approximated by manual docking of EACA at the binding site, followed by restrained energy minimization. With the RMS differences averaging variously between 1.0 and 1.5 Å, neither NMR structure appears to be as precise as the crystallographically determined one. Poorly defined Arg34 and Arg70 residues, however, are somewhat in agreement with the present work. But the ligand contacts of the modeled $K1_{Pg}$/EACA NMR structure with the anionic (3.5 Å) and the cationic (5.2 Å) centers are considerably larger than the X-ray result (Table 4). This is most likely the result of a kinked conformation modeled for EACA (Rejante & Llinas, 1994), with a dipole length of 6.5 Å, which is much smaller than that of 7.5 Å, reported here.

In summary, analysis of the conclusions previously drawn from site-directed mutagenesis approaches of studying the binding of EACA and AMCHA to $K1_{Pg}$, relative to predictions of ligand binding details that can be drawn from the crystal structures of the two $K1_{Pg}$/ligand complexes, shows that excellent agreement occurs between the two widely disparate methods of structural analysis. Thus, molecular details of this important binding process are becoming generally understood, a fact that allows for rational design to future experimentation targeted at developing more potent antifibrinolytic agents through redesign of both the ligand and the kringle domain and provides a focus to investigations aimed at a more thorough understanding of one of the most fundamental of biochemical events, protein/ligand binding.

REFERENCES

Bok, R. A., & Mangel, W. F. (1985) *Biochemistry 24*, 3279−3286.

Brunger, A. T. (1990) *X-PLOR Manual, Version 2.1*, Yale University, New Haven, CT.

Carter, C. W., Jr., & Carter, C. W. (1979) *J. Biol. Chem. 254*, 12219−12223.

Castellino, F. J. (1995) in *Molecular Basis of Thrombosis and Hemostasis* (High, K. A., & Roberts, H. R., Eds.) pp 495−515, Marcel Dekker, Inc., New York, NY.

Cudney, R., Patel, S., Weisgraber, K., Newhouse, Y., & McPherson, A. (1994) *Acta Crystallogr. D50*, 414−423.

De Marco, A., Motta, A., Llinas, M., & Laursen, R. A. (1986) *Arch. Biochem. Biophys. 244*, 727−741.

De Marco, A., Petros, A. M., Laursen, R. A., & Llinas, M. (1987) *Eur. Biophys. J. 14*, 359−368.

De Marco, A., Petros, A. M., Llinas, M., Kaptein, R., & Boelens, R. (1989) *Biochim. Biophys. Acta 994*, 121−137.

De Serrano, V. S., & Castellino, F. J. (1992a) *Biochemistry 31*, 11698−11706.

De Serrano, V. S., & Castellino, F. J. (1992b) *Biochemistry 31*, 3326−3335.

De Serrano, V. S., & Castellino, F. J. (1993) *Biochemistry 32*, 3540−3548.

De Serrano, V. S., Sehl, L. C., & Castellino, F. J. (1992) *Arch. Biochem. Biophys. 292*, 206−212.

de Vos, A. M., Ultsch, M. H., Kelley, R. F., Padmanbhan, K., Tulinsky, A., Westbrook, M. L., & Kossiakoff, A. A. (1992) *Biochemistry 31*, 270−279.

Finzel, B. C. (1987) *J. Appl. Crystallogr. 20*, 53−55.

Hendrickson, W. A. (1985) *Methods Enzymol. 115B*, 252−270.

Hoover, G. J., Menhart, N., Martin, A., Warder, S., & Castellino, F. J. (1993) *Biochemistry 32*, 10936−10943.

Jancarik, J., & Kim, S. H. (1991) *J. Appl. Crystallogr. 24*, 409−411.

Lee, B., & Richards, F. M. (1971) *J. Mol. Biol. 55*, 379−400.

Lerch, P. G., & Rickli, E. E. (1980) *Biochim. Biophys. Acta 625*, 374−378.

Lijnen, H. R., Hoylaerts, M., & Collen, D. (1980) *J. Biol. Chem. 255*, 10214−10222.

Llinas, M., Motta, A., De Marco, A., & Laursen, R. A. (1985) *J. Biosci. 8*, 121−129.
Magnusson, S., Petersen, T. E., Sottrup-Jensen, L., & Claeys, H. (1975) in *Proteases and Biological Control* (Reich, E., Rifkin, D. B., & Shaw, E., Eds.) pp 123−149, Cold Spring Harbor Laboratories, Cold Spring Harbor, NY.
Marti, D., Schaller, J., Ochensberger, B., & Rickli, E. E. (1994) *Eur. J. Biochem. 219*, 455−462.
McCance, S. G., Menhart, N., & Castellino, F. J. (1994) *J. Biol. Chem. 269*, 32405−32410.
McMullen, B. A., & Fujikawa, K. (1985) *J. Biol. Chem. 260*, 5328−5341.
Menhart, N., Sehl, L. C., Kelley, R. F., & Castellino, F. J. (1991) *Biochemistry 30*, 1948−1957.
Miles, L. A., Dahlberg, C. M., & Plow, E. F. (1988) *J. Biol. Chem. 263*, 11928−11934.
Moroi, M., & Aoki, N. (1976) *J. Biol. Chem. 251*, 5956−5965.
Mulichak, A. M., Tulinsky, A., & Ravichandran, K. G. (1991) *Biochemistry 30*, 10576−10588.
Navaza, J. (1994) *Acta Crystallogr. A50*, 157−163.
Nielsen, P. R., Einer-Jensen, K., Hotlet, T. L., Andersen, B. D., Poulsen, F. M., & Thogersen, H. C. (1993) *Biochemistry 32*, 13019−13025.
Novokhatny, V. V., Matsuka, Y. V., & Kudinov, S. A. (1989) *Thromb. Res. 53*, 243−252.
Padmanabhan, K., Wu, T. P., Ravichandran, K. G., & Tulinsky, A. (1994) *Protein Sci. 3*, 898−910.
Pennica, D., Holmes, W. E., Kohr, W. J., Harkins, R. N., Vehar, G. A., Ward, C. A., Bennett, W. F., Yelverton, E., Seeburg, P. H., Heyneker, H. L., Goeddel, D. V., & Collen, D. (1983) *Nature (London) 301*, 214−221.
Petros, A. M., Ramesh, V., & Llinas, M. (1989) *Biochemistry 28*, 1368−1376.
Rejante, M. R., & Llinas, M. (1994) *Eur. J. Biochem. 221*, 939−949.
Sehl, L. C., & Castellino, F. J. (1990) *J. Biol. Chem. 265*, 5482−5486.
Sottrup-Jensen, L., Claeys, H., Zajdel, M., Petersen, T. E., & Magnusson, S. (1978) *Prog. Chem. Fibrinolysis Thrombolysis 3*, 191−209.
Steffens, G. J., Gunzler, W. A., Otting, F., Frankus, E., & Flohe, L. (1982) *Hoppe-Seyler's Z. Physiol. Chem. 363*, 1043−1058.
Thewes, T., Constantine, K., Byeon, I.-J. L., & Llinas, M. (1990) *J. Biol. Chem. 265*, 3906−3915.
Trexler, M., Vali, Z., & Patthy, L. (1982) *J. Biol. Chem. 257*, 7401−7406.
Trexler, M., Banyai, L., Patthy, L., Pluck, N. D., & Williams, R. J. P. (1985) *Eur. J. Biochem. 152*, 439−446.
Tulinsky, A., & Blevins, R. A. (1986) *Acta Crytallogr. B42*, 198−200.
Tulinsky, A., Park, C. H., Mao, B., & Llinas, M. (1988) *Proteins: Struct., Funct., Genet. 3*, 85−96.
Vali, Z., & Patthy, L. (1984) *J. Biol. Chem. 259*, 13690−13694.
Varadi, A., & Patthy, L. (1983) *Biochemistry 22*, 2440−2446.
Varadi, A., & Patthy, L. (1984) *Biochemistry 23*, 2108−2112.
Weening-Verhoeff, E. J. D., Quax, P. H. A., van Leeuwen, R. T. J., Rehberg, E. F., Mariotti, K. R., & Verheijen, J. H. (1990) *Protein Eng. 4*, 191−198.
Wiman, B., & Wallen, P. (1977) *Thromb. Res. 10*, 213−222.
Wu, T.-P., Padmanabhan, K., Tulinsky, A., & Mulichak, A. M. (1991) *Biochemistry 30*, 10589−10594.
Wu, T. P., Padmanabhan, K. P., & Tulinsky, A. (1994) *Blood Coagulation Fibrinolysis 5*, 157−166.

BI9521351